

Transformer-CNN Cohort: Semi-supervised Semantic Segmentation by the Best of Both Students

Xu Zheng^{3*}, Yunhao Luo^{4*}, Hao Wang⁵, Chong Fu³ and Lin Wang^{1, 2 ‡}

¹ AI Thrust, HKUST(GZ)

² Dept. of CSE, HKUST

³ Northeastern University

⁴ Brown University

⁵ Alibaba Group

zhengxu128, devinluo27@gmail.com, cashenry@126.com, fuchong@mail.neu.edu.cn, linwang@ust.hk

Abstract

The popular methods for semi-supervised semantic segmentation mostly adopt a unitary network model using convolutional neural networks (CNNs) and enforce consistency of the model’s predictions over small perturbations applied to the inputs or model. However, such a learning paradigm suffers from a) limited learning capability of the CNN-based model; b) limited capacity of learning the discriminative features for the unlabeled data; c) limited learning for both global and local information from the whole image. In this paper, we propose a novel Semi-supervised Learning approach, called Transformer-CNN Cohort (TCC), that consists of two students with one based on the vision transformer (ViT) and the other based on the CNN. Our method subtly incorporates the multi-level consistency regularization on the predictions and the heterogeneous feature spaces via pseudo labeling for the unlabeled data. First, as the inputs of the ViT student are image patches, the feature maps extracted encode crucial class-wise statistics. To this end, we propose class-aware feature consistency distillation (CFCD) that first leverages the outputs of each student as the pseudo labels and generates class-aware feature (CF) maps. It then transfers knowledge via the CF maps between the students. Second, as the ViT student has more uniform representations for all layers, we propose consistency-aware cross distillation to transfer knowledge between the pixel-wise predictions from the cohort. We validate the TCC framework on Cityscapes and Pascal VOC 2012 datasets, which significantly outperforms existing semi-supervised methods by a large margin.

Introduction

Semantic segmentation (Long, Shelhamer, and Darrell 2015) is a computer vision task aiming to generate pixel-wise category prediction of an image. Most of the state-of-the-art (SoTA) methods focus on exploring the potential of convolutional neural networks (CNNs) and learning strategies (Ronneberger, Fischer, and Brox 2015; Wang et al. 2020a). However, a hurdle of training these models is the lack of large-scale and high-quality annotated datasets, imposing much burden for real applications, *e.g.*, autonomous driving (Yang et al. 2018). Consequently, growing attention

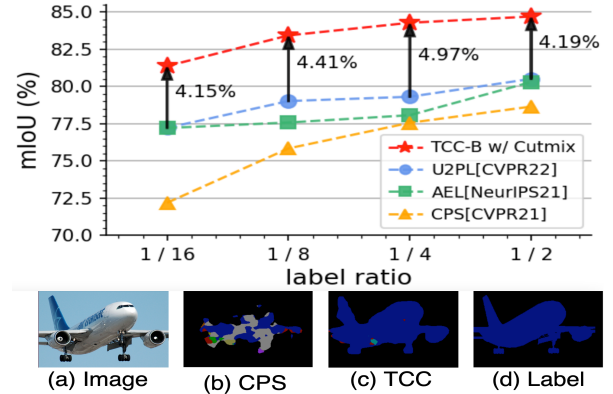


Figure 1: **Improvement over SoTA baseline** on the PASCAL VOC val set. Our TCC demonstrates a noticeable improvement over previous methods, *e.g.*, CPS (Chen et al. 2021b).

has been paid to deep semi-supervised learning (SSL) for semantic segmentation (Chen et al. 2021b) using the labeled data and additional unlabeled data.

The dominant deep SSL methods rely on consistency regularization (Tarvainen and Valpola 2017; Ke et al. 2019), pseudo labeling (Filipiak, Tempczyk, and Cygan 2021), entropy minimization (Grandvalet, Bengio et al. 2005) and bootstrapping (Grezl and Karafiát 2013), etc. However, these methods are only limited to classification, and their applications to semantic segmentation are still restricted (Ouali, Hudelot, and Tami 2020b). Only recently, attempts have been made focusing on consistency-based SSL for semantic segmentation (Mittal, Tatarchenko, and Brox 2019). In these methods, the ‘Teacher-Student’ structure is often explored by creating a teacher model and a student model either explicitly or implicitly (Zhang et al. 2021; Wang and Yoon 2021). The core spirit is to impose consistency on the predictions between two models via an exponential moving average (EMA) of the student and force the unlabeled data to meet the smooth assumption in SSL.

However, such a learning paradigm suffers from three key problems. First, using the isomorphic CNN-based models show limited learning capability of consistency regularization (See Tab. 1). Previous works leveraged perturba-

*Work done during internships; ‡ Corresponding author.

tions (French et al. 2019), different initialization (Ke et al. 2019) or different network structures (Luo et al. 2021) to impose model diversity. However, as the two feature extractors are inevitably coupled, it is difficult for them to extract complementary features in the later stage of training. Moreover, existing SSL methods merely leverage the pixel-wise predictions from CNNs, thus leading to a waste of rich inner knowledge in the feature space. Lastly, the input setting for SSL is always the entire image, making it difficult to learn both global and local (*i.e.*, long-range) semantic information although operated by strong data augmentation.

It has been shown that the Vision Transformer (ViT) can achieve comparable or even superior performance on image recognition tasks at a large scale (Dosovitskiy et al. 2020). Differing from CNNs consisting of convolutions (Convs), ViT’s basic computational paradigm is multi-head self-attentions (MHSA). Park et al. (Park and Kim 2021) show that MSAs and Convs exhibit opposite behaviors. That is, there exist surprisingly clear differences in the features and internal structures of ViT and CNN (Raghu et al. 2021).

Inspired by the success of ViT and ‘Dual-Student’ (Ke et al. 2019) in SSL for visual recognition, in this paper, we explore the potential of ViT and CNNs to tackle the above-mentioned problems for semi-supervised semantic segmentation. However, bringing the ViT to SSL is challenging because: *a)* the inner feature and output paradigm of ViT is heterogeneous from those of CNNs; *b)* the high-performance of ViT needs the pre-training with hundreds of millions of annotated images using a large infrastructure (Touvron et al. 2021); *c)* in SSL, how to make Convs and MSAs learn with each other for the *unlabeled* data from the feature and image level needs to be explored.

To this end, we propose, to the best of our knowledge, the *first* yet novel SSL method for semantic segmentation, called Transformer-CNN Cohort (TCC), by *subtly incorporating the multi-level distillation to add consistency on the pixel-wise predictions and the heterogeneous feature space via pseudo labeling for the unlabeled data*. Specifically, as the ViT and CNN students have different input and inner feature flow forms, we notice that the feature maps extracted encode crucial complementary class-wise statistics (Wang et al. 2020b). Therefore, we propose class-aware feature consistency distillation (CFCD) that first leverages the output of each student as the pseudo labels and generates pseudo prototype maps. Importantly, it is also the *first* time that we explore pseudo labeling in SSL to facilitate feature distillation for the unlabeled data. The class-aware feature (CF) maps are computed by averaging the features on all pixels having the same pseudo labels. Class-aware feature variation knowledge is transformed via the CF maps between the cohort. Moreover, as the ViT student has more uniform representations for all layers, we propose Consistency-aware Cross Distillation (CCD) to distill knowledge based on the pixel-wise predictions from the cohort. As such, we can reduce the large amount of training data required for ViT and accommodate ViT to SSL tasks with high performance. We conduct extensive experiments with various settings on two benchmark datasets: PASCAL VOC 2012 (Everingham et al.) and Cityscapes (Cordts et al. 2016). The experimental

results show that our TCC framework surpasses the existing SoTA methods by 4.15% under 1/16 label ratio on POASCAL VOC 2012 dataset and 1.03% under 1/16 partition protocols on the CityScapes dataset, as shown in Fig. 1.

In summary, the contributions of our paper are four-fold. (I) We propose the first SSL framework, with the transformer-CNN cohort, that imposes multi-level consistency on the pixel-wise predictions and the heterogeneous feature space. (II) We propose CFCD to distill the complementary class-wise feature knowledge via pseudo labeling for the *unlabeled data*. Notably, we are also the *first* to explore pseudo labeling for feature distillation in semi-supervised segmentation. (III) We propose CCD to distill the pixel-wise prediction knowledge to impose consistency for the students in the cohort. (IV) Our TCC framework achieves *new* SoTA performance on both benchmarks.

Related work

Semi-supervised Learning The mainstream SSL methods rely on consistency regularization (Tarvainen and Valpola 2017), pseudo labeling (Filipiak, Tempczyk, and Cygan 2021), entropy minimization (Grandvalet, Bengio et al. 2005) and bootstrapping (Grezl and Karafiát 2013), transductive models (Gammerman, Vovk, and Vapnik 2013; Joachims 2003, 1999), graph-based methods (Lin, Gao, and Li 2019; Li et al. 2019; Liu et al. 2019), generative models (Kingma et al. 2014; Odena 2016; Souly, Spampinato, and Shah 2017). We refer readers to (Ouali, Hudehot, and Tami 2020a) for more details. Consistency training methods (Sajjadi, Javanmardi, and Tasdizen 2016; Miyato et al. 2018; Verma et al. 2019; Abuduweili et al. 2021; Lee et al. 2022; Saito, Kim, and Saenko 2021) typically add perturbations (*i.e.*, noise) to the unlabeled data, among which some adopt the ‘Teacher-Student’ structure (Lee et al. 2013). Pseudo labeling (Rosenberg, Hebert, and Schneiderman 2005; Bachman, Alsharif, and Precup 2014; Zou et al. 2020; Arazo et al. 2019; Xiong et al. 2021) generates labels for unlabeled data to enrich training data. Recently, some methods (Berthelot et al. 2019b,a) combine consistency regularization and pseudo labeling based on the predictions. We focus on more challenging semantic segmentation by exploring the potential of ViT and CNNs. Our TCC framework subtly imposes the multi-level consistency distillation on the pixel-wise predictions and the heterogeneous feature space via pseudo labeling for the unlabeled data.

Semi-supervised Semantic Segmentation. Consistency regularization is widely applied for semi-supervised segmentation (Sohn et al. 2020). The key insight of this branch of approaches is that the predictions or intermediate features should be consistent across different semantic-preserving transformations on input or model of the same data. The image-level perturbation methods, *e.g.*, (French et al. 2019) randomly augment the input images while the feature-level perturbation methods, *e.g.*, (Ke et al. 2020) uses a multi-decoder strategy to augment the features. Moreover, CPS (Chen et al. 2021b) enforces consistency by using the pseudo segmentation maps with additional benefits like expanding the training data. In addition, generative adversarial networks (GANs) are also adopted for SSL (Hung

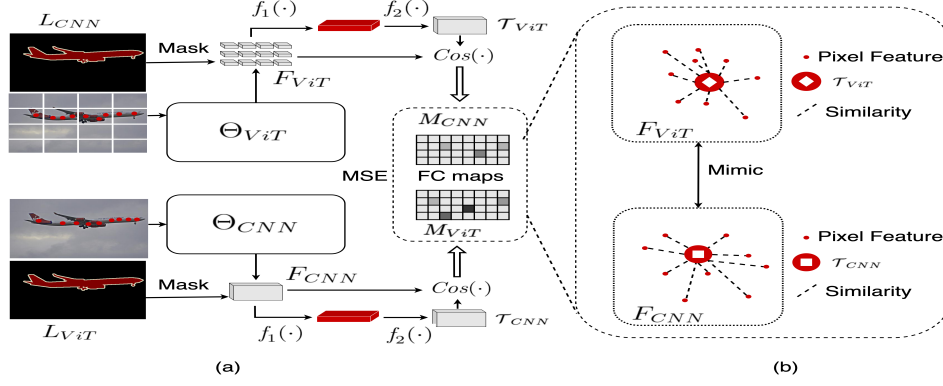


Figure 3: (a) Overview of the proposed CFCD. (b) shows the two networks are endowed with different class-wise feature variations, which can be characterized as the set of similarities (dash lines) between the feature on each pixel and its corresponding class-wise prototype. We make the $f(\theta_{ViT})$ and $f(\theta_{CNN})$ learn from each other as the higher similarity means lower variation.

$f(X; \theta_{CNN})$, which can be formulated as:

$$\begin{aligned} L_{CNN}, P_{CNN}, F_{CNN} &= f(X; \theta_{CNN}); \\ L_{ViT}, P_{ViT}, F_{ViT} &= f(X; \theta_{ViT}). \end{aligned} \quad (1)$$

Our key ideas are three folds. Firstly, as $f(X; \theta_{ViT})$ and $f(X; \theta_{CNN})$ have different inputs and inner feature forms, the extracted feature maps encode crucial complementary class-wise statistics. Therefore, we propose class-aware feature consistency distillation (CFCD) that first leverages the output of each student as the pseudo labels and generates feature prototype maps. Note that it is the *first time we explore pseudo labelling in SSL to facilitate feature distillation for the unlabeled data*. The class-aware features maps are computed by averaging the features on all pixels having the same pseudo labels. Feature variation knowledge is transformed via the cohort’s class-aware feature (CF) maps. Secondly, as $f(X; \theta_{ViT})$ possesses more uniform representations for all layers (Raghu et al. 2021), we propose Consistency-aware Cross Distillation (CCD) that distills the pixel-wise prediction information bidirectionally based on the heterogeneous students. Lastly, similar to other SSL approaches, e.g., (Sohn et al. 2020), supervised training also is applied to both $(X; \theta_{ViT})$ and $f(X; \theta_{CNN})$ for the limited labeled data. We now describe these components in detail.

Class-aware Feature Consistency Distillation

Pseudo Prototype Theoretically, high-dimensional feature representations obtained by two different models should be distinct explicitly but share implicit commonalities (Wang et al. 2020b). For all pixels of the same class in the corresponding class-wise label maps, their mapping center in feature space is referred to as the class-wise prototype. *This prototype is based on the condition that all pixels belonging to the same class should coincide in feature mapping space.* However, the feature maps of all pixels of the same class may not fall on the prototype completely; therefore, we estimate the class-aware feature variation to measure the similarity between the mapping of each pixel and the prototype. The class-aware feature variation for pixels can be obtained from the predictions and the inner features of $f(X; \theta_{ViT})$

and $f(X; \theta_{CNN})$. As features reflect how students in the cohort understand the input, it is crucial that reliable prototype calculation is guaranteed. However, for the unlabeled data, there are no prior labels for computing the prototype in SSL; thus, we leverage the pseudo labels predicted from one student as the source prototype for the other. That is, the CF map obtained from $f(X; \theta_{ViT})$ is taken as the standard prototype for student $f(X; \theta_{CNN})$ in the feature space, and vice versa. As such, $f(X; \theta_{ViT})$ and $f(X; \theta_{CNN})$ can be better correlated to each other despite of the difference of computing paradigms (MHSA for $f(X; \theta_{ViT})$ and Convs for $f(X; \theta_{CNN})$).

As shown in Fig. 3, to impose class-aware feature consistency to both students in the cohort, pseudo labels are down-sampled with nearest neighbour interpolation to match the spatial size of the high-dimensional features. Then, average pooling is operated on the masked features, corresponding to pixels with the same label for each class to get the class-wise pseudo prototype. Finally, we perform average pooling on the masked region of each pseudo prototype to ensure each position stores the corresponding high-dimensional feature of the class-wise prototype. Overall, the prototype can be formulated as:

$$\begin{aligned} \mathcal{T}_{ViT} &= f_2(f_1(\text{Mask}(F_{ViT}, L_{CNN}))); \\ \mathcal{T}_{CNN} &= f_2(f_1(\text{Mask}(F_{CNN}, L_{ViT}))), \end{aligned} \quad (2)$$

where \mathcal{T}_{ViT} and \mathcal{T}_{CNN} denote the pseudo prototypes for the students $f(X; \theta_{ViT})$ and $f(X; \theta_{CNN})$, respectively; $f_1(\cdot)$ is the average pooling; $f_2(\cdot)$ is the unpooling operation; F_{ViT} and F_{CNN} are the high-dimensional features masked by pseudo label maps L_{CNN} and L_{ViT} , respectively. As such, we can obtain CF maps via calculating the similarity, e.g., cosine similarity, between \mathcal{T}_{CNN} and \mathcal{T}_{CNN} for each student, as shown in Fig. 3. More details of CF map calculation will be described in the following section.

Feature Distillation via Pseudo Prototype The CNN kernel of $f(X; \theta_{CNN})$ inspects adjacent pixels and gradually expands its receptive field to a more significant portion of an image, producing features with high locality. By contrast, $f(X; \theta_{ViT})$ manipulates patch-level image at every

Method	Backbone	Label Rate			
		1/16(662)	1/8(1323)	1/4(2646)	1/2(5291)
MT (Tarvainen and Valpola 2017)	ResNet-50	66.77	70.78	73.22	75.41
	ResNet-101	70.59	73.20	76.62	77.61
CCT (Ouali, Hudelot, and Tami 2020b)	ResNet-50	65.22	70.87	73.43	74.75
	ResNet-101	67.94	73.00	76.17	77.56
CPS (Chen et al. 2021b)	ResNet-50	68.21	73.20	74.24	75.91
	ResNet-101	72.18	75.83	77.55	78.64
n -CPS (Filipiak, Tempczyk, and Cygan 2021)	ResNet-50	68.36	73.45	75.75	77.00
	ResNet-101	73.51	76.46	78.59	79.90
AEL (Hu et al. 2021)	ResNet-101	77.20	77.57	78.06	80.29
ST++ (Yang et al. 2022)	ResNet-50	73.20	75.50	76.00	-
	ResNet-101	74.70	77.90	77.90	-
U2PL (Wang et al. 2022)	ResNet-101	77.21	79.01	79.30	80.50
ELN (Kwon and Kwak 2022)	ResNet-50	70.52	73.20	74.63	-
	ResNet-101	72.52	75.10	76.58	-
Ours	TCC-S	79.16	80.28	82.32	82.52
	w/ Cutmix	81.35	83.05	83.55	84.04
	TCC-B	80.17	81.17	82.42	82.80
	w/ Cutmix	81.36	83.42	84.27	84.29

Table 1: **Comparison with state-of-the-arts** on the PASCAL VOC 2012 val set under different partition protocols. All the methods are based on DeepLabv3+. (TCC-B: TCC-Base; TCC-S: TCC-Small; w/ Cutmix: with cutmix augmentation)

stage, having a global vision even at the beginning. Though the two models achieve similar performance after the training, their learning process is distinctive. Moreover, the feature maps extracted from them encode vital complementary class-wise statistics. Intuitively, we find that transferring the feature-level knowledge can complement the drawbacks of each model and thus yield better results. Inspired by (Wang et al. 2020b), we apply consistency regularization on the pseudo feature variation between $f(X; \theta_{ViT})$ and $f(X; \theta_{CNN})$, as depicted in Fig. 3. Especially, we extract the high-dimensional features output from the last stage of $f(X; \theta_{ViT})$ and $f(X; \theta_{CNN})$ to calculate their corresponding class-wise prototype. The prototype \mathcal{T} at pixel p of class c is computed by averaging the features on all pixels having class label c , given by Eq. 3:

$$\mathcal{T}(i) = \frac{1}{|S_c|} \sum_{i \in S_c} f(i) \quad (3)$$

$$M(i) = \text{Cos}(f(i), \mathcal{T}(i)); \quad (4)$$

where $f(i)$ denotes the feature on pixel i , S_c is the set of pixels having the label c , $|S_c|$ stands for the size of the set S_c , $\mathcal{T}(i)$ is the class-wise feature variation map from its cohort, and $M(i)$ denotes the value of class-wise feature variation map at pixel i . In Eq. 4, due to the intrinsic difference (e.g., magnitude, deviation) in the feature maps between $f(X; \theta_{ViT})$ and $f(X; \theta_{CNN})$, we adopt the cosine similarity $\text{Cos}(\cdot)$ to better formulate the relative distribution for each class. Finally, the CFCD loss \mathcal{L}_f minimizes the distance between feature variation maps of the students $f(X; \theta_{ViT})$ and $f(X; \theta_{CNN})$. Specifically, we employ the Mean Squared Error (MSE) loss as follows:

$$\mathcal{L}_f = \frac{1}{N} \sum_{p \in \Omega} (M_{CNN}(i) - M_{ViT}(i))^2, \quad (5)$$

where N is the total numbers of pixels, Ω denotes the image, $M_{CNN}(p)$ and $M_{ViT}(p)$ represent the corresponding pseudo feature variation map of the CNN and ViT students.

Consistency-aware Cross Distillation

Though $f(\theta_{ViT})$ and $f(\theta_{CNN})$ share different learning capacities for the unlabeled data D_u , their predictions should be consistent according to the *smoothness assumption* where samples in the same cluster are expected to have the same labels. In particular, instead of using the Exponential Moving Average (Tarvainen and Valpola 2017) to update the predictions, we find that measuring the cross-model discrepancy between $f(\theta_{ViT})$ and $f(\theta_{CNN})$ helps improve each student’s representations. Accordingly, we propose Consistency-aware Cross Distillation (CCD) to enforce consistency between the outputs of the cohort to extract additional information for the unlabeled data D_u . CCD is bidirectional: one is from $f(\theta_{CNN})$ to $f(\theta_{ViT})$ and the other one is from $f(\theta_{ViT})$ to $f(\theta_{CNN})$. That is, we use the logits output P_{CNN} from the CNN student $f(\theta_{CNN})$ to supervise the logits output P_{ViT} of the ViT student $f(\theta_{ViT})$, and vice versa. The CCD loss on the unlabeled data D_u can be written as:

$$\mathcal{L}_d^u = \frac{1}{|D_l|} (\mathcal{L}_{kl}(P_{CNN}, P_{ViT}) + \mathcal{L}_{kl}(P_{ViT}, P_{CNN})), \quad (6)$$

where the \mathcal{L}_{kl} is the standard KL divergence. The CCD loss \mathcal{L}_d^l on the labeled data D_l can be defined in the same manner. The total CCD loss is the combination of losses on both the labeled D_l and unlabeled data D_u : $\mathcal{L}_d = \mathcal{L}_d^l + \mathcal{L}_d^u$.

Optimization

The algorithm for training our TCC framework is depicted in *Algorithm 1 in the suppl. material*. The training objective

Method	Backbone	Label Rate			
		1/16(662)	1/8(1323)	1/4(2646)	1/2(5291)
MT (Tarvainen and Valpola 2017)	ResNet-50	66.14	72.03	74.47	77.43
	ResNet-101	68.08	73.71	76.53	78.59
CCT (Ouali, Hudelot, and Tami 2020b)	ResNet-50	66.35	72.46	75.68	76.78
	ResNet-101	69.64	74.48	76.35	78.29
CPS (Chen et al. 2021b)	ResNet-50	69.79	74.39	76.85	78.64
	ResNet-101	70.50	75.71	77.41	80.08
3-CPS (Filipiak, Tempczyk, and Cygan 2021)	ResNet-101	75.86	77.99	78.95	80.26
AEL (Hu et al. 2021)	ResNet-101	75.83	77.90	79.01	80.28
ST++ (Yang et al. 2022)	ResNet-50	-	72.70	73.80	-
U^2 PL (Wang et al. 2022)	ResNet-101	70.30	74.37	76.47	79.05
ELN (Kwon and Kwak 2022)	ResNet-50	70.33	73.52	75.33	-
Ours	TCC-B	75.79	77.53	78.47	80.83
	w/ CutMix	76.89	78.52	80.04	80.93

Table 2: **Comparison with the state-of-the-arts** on the Cityscapes val set under different partition protocols. All the methods are based on DeepLabv3+. (TCC-B: TCC-Base; w/ Cutmix: with cutmix augmentation)

contains three losses as follows:

$$\mathcal{L} = \mathcal{L}_s + g(t) \cdot (\mathcal{L}_d + \lambda \mathcal{L}_f), \quad (7)$$

where the \mathcal{L}_s is supervised loss, the \mathcal{L}_d refers to the prediction-level CCD loss and the \mathcal{L}_f is the CFCD loss that measures the class-aware feature variation consistency between $f(\theta_{ViT})$ and $f(\theta_{CNN})$. The $g(t)$ is a consistency ramp up function following (Laine and Aila 2016), and λ is a fixed constant. The supervision loss \mathcal{L}_s is formulated using the standard Dice coefficient loss function on the labeled images over the heterogeneous ViT and CNN students:

$$\mathcal{L}_s = \frac{1}{|D_l|} \sum_{X \in D_l} (\mathcal{L}_{dice}(P_{CNN}, Y_{CNN}) + \mathcal{L}_{dice}(P_{ViT}, Y_{ViT})) \quad (8)$$

where \mathcal{L}_{dice} indicates the Dice coefficient loss function and Y are the ground truth (GT) labels.

Experiments and Evaluation

Datasets. *Pascal VOC* contains 20 foreground object classes plus an extra background class. The standard training, validation, and test sets consist of 1464, 1449, and 1456 images, respectively. We adopt the augmented set from (Hariharan et al. 2011) which contains 10582 images as our full training set. *Cityscapes* contains a diverse set of video sequences recorded in street scenes from 50 different cities, with high-quality pixel-level annotations. The official split has 2975 images for training, 500 for validation, and 1525 for testing. Each image in *Cityscapes* is finely annotated with pixel-level labels of 19 classes. We divide the whole training set into two groups via randomly sampling 1/2, 1/4, 1/8, and 1/16 of the whole set as labeled images and the rest as unlabeled images. Images in each set are the same as U^2 PL (Wang et al. 2022) (the SoTA method) for a fair comparison.

Evaluation. We leverage the mean Intersection-over-Union (mIOU) as an evaluation metric. Our trained models are evaluated on PASCAL VOC 2012 validation set (1456 images) and the *Cityscapes* validation set (500 images) via test-

ing at a single scale, respectively. We report the mIOU of the best model in the cohort.

Implementation details. We implement our TCC framework using Pytorch. We initialize the weights of two backbones, *i.e.*, the students $f(\theta_{ViT})$ and $f(\theta_{CNN})$, with the weights pre-trained on ImageNet 1K and the weights of two segmentation heads (of DeepLabv3+ (Chen et al. 2017)) randomly. For fair comparisons, two types of settings in our TCC are settled to be compared with ResNet-50 and ResNet-101, *i.e.*, Cohort-Small (TCC-S) and Cohort-Base (TCC-B). Specifically, *ResNet-50* and *PVT-S* are the two backbones in TCC-S, while *ConvNeXt-B* and *PVT-M* in TCC-B. We also report the results of ResNet, PVT, and ConvNext-based implementations of TCC in the ablation study.

Comparison with the SoTA methods

We compare our method with the SoTA semi-supervised methods including: Mean-Teacher(MT) (Tarvainen and Valpola 2017), Cross Consistency Training(CCT) (Ouali, Hudelot, and Tami 2020b), Cross Pseudo Supervision(CPS) (Chen et al. 2021b), AEL (Hu et al. 2021), ST++ (Yang et al. 2022), U^2 PL (Wang et al. 2022) and ELN (Kwon and Kwak 2022) under different label ratios.

Our method even outperforms *n*-CPS(Filipiak, Tempczyk, and Cygan 2021), a 3-model based SSL method, by 7.85%, 6.96%, 5.68%, and 4.90%, respectively, under the same labeled ratios on *Pascal VOC* dataset. The greatest improvement at the 1/16 label ratio indicates that the combination of CNN and ViT students can facilitate each other when learning unlabeled data and generalize well when learning labeled data, which is consistent with our assumption.

Detailed results by datasets. *PASCAL VOC 2012*: Tab. 1 shows the comparison results. On all label ratios (1/2, 1/4, 1/8, and 1/16), our TCC approach (w/o CutMix) consistently outperforms the other methods. And our TCC approach (w/ CutMix) achieves the best performance and sets new SoTA under all label ratios. With lower labeled ratios, our approach (w/ CutMix) outperforms the U^2 PL by 4.15% and 4.41%, respectively, under 1/16 and 1/8 label ratios. ***This confirms that using two heterogeneous models, i.e., ViT***

Losses			PASCAL VOC 2012			
\mathcal{L}_s	\mathcal{L}_d	\mathcal{L}_f	1/16(662)	1/8(1323)	1/4(2646)	1/2(5291)
✓			74.65	76.22	76.71	77.01
✓	✓		77.90	80.46	81.60	81.95
✓	✓	✓	80.17	81.17	82.42	82.80

Table 3: **Ablation study of different loss combinations** on PASCAL VOC 2012. The results are obtained with TCC-B under the 1/16, 1/8, 1/4, 1/2 data partition protocol and the observations are consistent for other partition protocols.

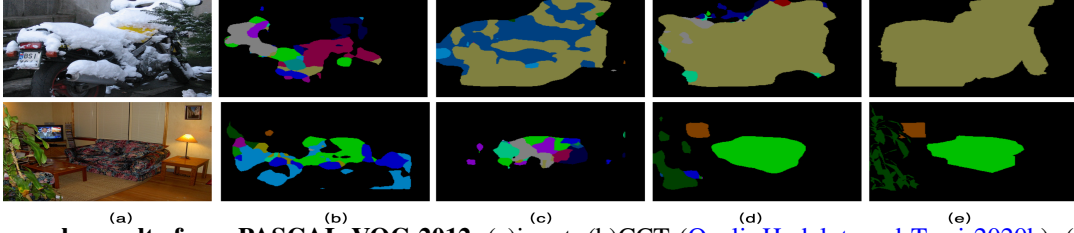


Figure 4: **Example results from PASCAL VOC 2012.** (a)input, (b)CCT (Ouali, Hudelot, and Tami 2020b), (c)CPS (Chen et al. 2021b), (d)ours, and (e) ground truth. All the approaches based on DeepLabv3+.

and CNN, in the consistency regularization approaches achieves better performance, especially with less annotated data. Fig. 4 shows the qualitative results with comparisons with CCT and CPS. CCT struggles to catch the main objects from inputs and wrongly classified many regions of interest into the background (black). It renders a colorful mask over a single object and is especially devastating if some natural camouflage exists, e.g., the snow-covered motorbike. CPS performs relatively better than CCT. It can roughly outline the boundary of objects of interest but the inner pixel-wise segmentation results are still heterogeneous for a single object. In stark contrast, our method achieves much neater and cleaner segmentation results (4th column), which is much closer to the GT label maps (5th column).

Cityscapes val set: Tab. 2 shows the quantitative results where our TCC approach consistently outperforms the SoTA methods. The improvements of mIOU of our method (w/o CutMix augmentation) over the 2-model baseline method (AEL) are 1.06%, 0.62%, 1.03%, 0.65% under label ratio of 1/16, 1/8, 1/4, and 1/2, respectively. *The qualitative results can be found in the suppl. material.*

Ablation study and Analysis

Loss functions. We conduct ablation experiments on the PASCAL VOC 2012 to analyze the impact of the CCD loss \mathcal{L}_d and CFCD loss \mathcal{L}_f in our TCC framework. In Tab. 3, different combinations of losses are applied. We can see that TCC framework leverages the unlabeled data well with an average improvement of 5.49% over fully supervised by labeled data. Both \mathcal{L}_d and \mathcal{L}_f contribute positively to the validation mIOU in every label rate. For example, in the 1/16 case, \mathcal{L}_d brings an increase of 3.25% in the mIOU and another 2.27% boost after the addition of \mathcal{L}_f . We notice that the increases brought by \mathcal{L}_f decline when the number of unlabeled data decreases. It is also intuitive since CF maps in \mathcal{L}_f is inferred by unlabeled data. Reduction of the hampers models fitting the actual class-wise feature variance distribution, thus lowering the improvement downward.

Varying backbone models. We conduct the ablation studies on the PASCAL VOC 2012 with 1/8 label rate to analyze

Method	Backbones	Label Ratio			
		1/16	1/8	1/4	1/2
U^2 PL	ResNet-101	77.21	79.01	79.30	80.50
	ResNet-50	77.79	78.95	80.51	80.98
	PVT-M	71.12	73.84	74.44	76.72
Ours	ConvNext-B	78.92	80.15	80.81	80.95
	TCC-S	79.16	80.28	82.32	82.52
	TCC-B	80.17	81.17	82.42	82.80

Table 4: **Ablation of our TCC with different backbones** on the PASCAL VOC 2012 val set. All the methods are based on DeepLabv3+.

the impact of the changing backbones, including ResNet, PVT, ConvNext and our TCC. Tab. 4 shows that our cohort can better promote the segmentation performance under the dual-student network structure in SLL. We fully explore the potential of heterogeneous computing paradigms (MSAs and Convs) via FVCD in the feature space and CCD on the prediction. This way, we successfully introduce ViT into the semi-supervised semantic segmentation task. *Additional comparisons with the fully supervised baselines and few-shot supervision can be found in the suppl. material.*

Conclusion

In this paper, we proposed TCC, a novel framework for semi-supervised semantic segmentation by exploring the best of both students. Our method subtly incorporates the multi-level consistency regularization on both the predictions and the heterogeneous feature space via pseudo labeling for the unlabeled data. First, the feature variation knowledge is transformed via CF maps between the cohort. Second, we also proposed to distill knowledge from the pixel-wise predictions based on the heterogeneous students. The proposed TCC framework significantly outperformed the SoTA semi-supervised methods by a large margin.

For the future direction, we plan to further explore the dual-student framework with more heterogeneous models for semi-supervised semantic segmentation.

References

- Abuduweili, A.; Li, X.; Shi, H.; Xu, C.-Z.; and Dou, D. 2021. Adaptive Consistency Regularization for Semi-Supervised Transfer Learning. In *Proceedings of the IEEE/CVF Conference on Computer Vision and Pattern Recognition (CVPR)*, 6923–6932.
- Arazo, E.; Ortego, D.; Albert, P.; O’Connor, N. E.; and McGuinness, K. 2019. Pseudo-Labeling and Confirmation Bias in Deep Semi-Supervised Learning. *CoRR*, abs/1908.02983.
- Bachman, P.; Alsharif, O.; and Precup, D. 2014. Learning with Pseudo-Ensembles. *arXiv:1412.4864*.
- Bao, H.; Dong, L.; and Wei, F. 2021. BEiT: BERT Pre-Training of Image Transformers. *arXiv preprint arXiv:2106.08254*.
- Beal, J.; Kim, E.; Tzeng, E.; Park, D. H.; Zhai, A.; and Kisluyuk, D. 2020. Toward transformer-based object detection. *arXiv preprint arXiv:2012.09958*.
- Berthelot, D.; Carlini, N.; Cubuk, E. D.; Kurakin, A.; Sohn, K.; Zhang, H.; and Raffel, C. 2019a. ReMixMatch: Semi-Supervised Learning with Distribution Alignment and Augmentation Anchoring. *CoRR*, abs/1911.09785.
- Berthelot, D.; Carlini, N.; Goodfellow, I.; Papernot, N.; Oliver, A.; and Raffel, C. A. 2019b. MixMatch: A Holistic Approach to Semi-Supervised Learning. In Wallach, H.; Larochelle, H.; Beygelzimer, A.; d’Alché-Buc, F.; Fox, E.; and Garnett, R., eds., *Advances in Neural Information Processing Systems*, volume 32. Curran Associates, Inc.
- Chen, H.; Wang, Y.; Guo, T.; Xu, C.; Deng, Y.; Liu, Z.; Ma, S.; Xu, C.; Xu, C.; and Gao, W. 2021a. Pre-trained image processing transformer. In *Proceedings of the IEEE/CVF Conference on Computer Vision and Pattern Recognition*, 12299–12310.
- Chen, L.-C.; Papandreou, G.; Kokkinos, I.; Murphy, K.; and Yuille, A. L. 2017. Deeplab: Semantic image segmentation with deep convolutional nets, atrous convolution, and fully connected crfs. *IEEE transactions on pattern analysis and machine intelligence*, 40(4): 834–848.
- Chen, X.; Yuan, Y.; Zeng, G.; and Wang, J. 2021b. Semi-Supervised Semantic Segmentation with Cross Pseudo Supervision. In *Proceedings of the IEEE/CVF Conference on Computer Vision and Pattern Recognition*, 2613–2622.
- Cordts, M.; Omran, M.; Ramos, S.; Rehfeld, T.; Enzweiler, M.; Benenson, R.; Franke, U.; Roth, S.; and Schiele, B. 2016. The Cityscapes Dataset for Semantic Urban Scene Understanding. In *Proc. of the IEEE Conference on Computer Vision and Pattern Recognition (CVPR)*.
- Dai, Z.; Cai, B.; Lin, Y.; and Chen, J. 2021. Up-detr: Unsupervised pre-training for object detection with transformers. In *Proceedings of the IEEE/CVF Conference on Computer Vision and Pattern Recognition*, 1601–1610.
- Dosovitskiy, A.; Beyer, L.; Kolesnikov, A.; Weissenborn, D.; Zhai, X.; Unterthiner, T.; Dehghani, M.; Minderer, M.; Heigold, G.; Gelly, S.; et al. 2020. An image is worth 16x16 words: Transformers for image recognition at scale. *arXiv preprint arXiv:2010.11929*.
- Everingham, M.; Van Gool, L.; Williams, C. K. I.; Winn, J.; and Zisserman, A. 2012. The PASCAL Visual Object Classes Challenge 2012 (VOC2012) Results. <http://www.pascal-network.org/challenges/VOC/voc2012/workshop/index.html>.
- Feng, Z.; Zhou, Q.; Cheng, G.; Tan, X.; Shi, J.; and Ma, L. 2020. Semi-supervised semantic segmentation via dynamic self-training and classbalanced curriculum. *arXiv preprint arXiv:2004.08514*, 1(2): 5.
- Filipiak, D.; Tempczyk, P.; and Cygan, M. 2021. n -CPS: Generalising Cross Pseudo Supervision to n networks for Semi-Supervised Semantic Segmentation. *arXiv preprint arXiv:2112.07528*.
- French, G.; Laine, S.; Aila, T.; Mackiewicz, M.; and Finlayson, G. 2019. Semi-supervised semantic segmentation needs strong, varied perturbations. *arXiv preprint arXiv:1906.01916*.
- Gamerman, A.; Vovk, V.; and Vapnik, V. 2013. Learning by Transduction. *arXiv:1301.7375*.
- Grandvalet, Y.; Bengio, Y.; et al. 2005. Semi-supervised learning by entropy minimization. *CAP*, 367: 281–296.
- Grezl, F.; and Karafiát, M. 2013. Semi-supervised bootstrapping approach for neural network feature extractor training. In *2013 IEEE Workshop on Automatic Speech Recognition and Understanding*, 470–475. IEEE.
- Hariharan, B.; Arbeláez, P.; Bourdev, L.; Maji, S.; and Malik, J. 2011. Semantic contours from inverse detectors. In *2011 international conference on computer vision*, 991–998. IEEE.
- Hinton, G.; Vinyals, O.; and Dean, J. 2015. Distilling the knowledge in a neural network. *arXiv preprint arXiv:1503.02531*.
- Hu, H.; Wei, F.; Hu, H.; Ye, Q.; Cui, J.; and Wang, L. 2021. Semi-supervised semantic segmentation via adaptive equalization learning. *Advances in Neural Information Processing Systems*, 34: 22106–22118.
- Hung, W.-C.; Tsai, Y.-H.; Liou, Y.-T.; Lin, Y.-Y.; and Yang, M.-H. 2018. Adversarial learning for semi-supervised semantic segmentation. *arXiv preprint arXiv:1802.07934*.
- Ibrahim, M. S.; Vahdat, A.; Ranjbar, M.; and Macready, W. G. 2020. Semi-supervised semantic image segmentation with self-correcting networks. In *Proceedings of the IEEE/CVF conference on computer vision and pattern recognition*, 12715–12725.
- Joachims, T. 1999. Transductive Inference for Text Classification Using Support Vector Machines. In *Proceedings of the Sixteenth International Conference on Machine Learning, ICML ’99*, 200–209. San Francisco, CA, USA: Morgan Kaufmann Publishers Inc. ISBN 1558606122.
- Joachims, T. 2003. Transductive Learning via Spectral Graph Partitioning. 290–297.
- Ke, Z.; Qiu, D.; Li, K.; Yan, Q.; and Lau, R. W. 2020. Guided collaborative training for pixel-wise semi-supervised learning. In *European conference on computer vision*, 429–445. Springer.

- Ke, Z.; Wang, D.; Yan, Q.; Ren, J.; and Lau, R. W. 2019. Dual student: Breaking the limits of the teacher in semi-supervised learning. In *Proceedings of the IEEE/CVF International Conference on Computer Vision*, 6728–6736.
- Kingma, D. P.; Rezende, D. J.; Mohamed, S.; and Welling, M. 2014. Semi-Supervised Learning with Deep Generative Models. *arXiv:1406.5298*.
- Kwon, D.; and Kwak, S. 2022. Semi-supervised Semantic Segmentation with Error Localization Network. In *Proceedings of the IEEE/CVF Conference on Computer Vision and Pattern Recognition*, 9957–9967.
- Laine, S.; and Aila, T. 2016. Temporal ensembling for semi-supervised learning. *arXiv preprint arXiv:1610.02242*.
- Lee, D.; Kim, S.; Kim, I.; Cheon, Y.; Cho, M.; and Han, W.-S. 2022. Contrastive Regularization for Semi-Supervised Learning. *arXiv preprint arXiv:2201.06247*.
- Lee, D.-H.; et al. 2013. Pseudo-label: The simple and efficient semi-supervised learning method for deep neural networks. In *Workshop on challenges in representation learning, ICML*, volume 3, 896.
- Li, Q.; Wu, X.-M.; Liu, H.; Zhang, X.; and Guan, Z. 2019. Label Efficient Semi-Supervised Learning via Graph Filtering. *2019 IEEE/CVF Conference on Computer Vision and Pattern Recognition (CVPR)*, 9574–9583.
- Lin, W.; Gao, Z.; and Li, B. 2019. Shoestring: Graph-Based Semi-Supervised Learning with Severely Limited Labeled Data. *CoRR*, abs/1910.12976.
- Liu, B.; Wu, Z.; Hu, H.; and Lin, S. 2019. Deep Metric Transfer for Label Propagation with Limited Annotated Data. In *Proceedings of the IEEE/CVF International Conference on Computer Vision (ICCV) Workshops*.
- Long, J.; Shelhamer, E.; and Darrell, T. 2015. Fully convolutional networks for semantic segmentation. In *Proceedings of the IEEE conference on computer vision and pattern recognition*, 3431–3440.
- Luo, X.; Hu, M.; Song, T.; Wang, G.; and Zhang, S. 2021. Semi-Supervised Medical Image Segmentation via Cross Teaching between CNN and Transformer. *arXiv preprint arXiv:2112.04894*.
- Mendel, R.; Souza, L. A. d.; Rauber, D.; Papa, J. P.; and Palm, C. 2020. Semi-supervised segmentation based on error-correcting supervision. In *European Conference on Computer Vision*, 141–157. Springer.
- Mittal, S.; Tatarchenko, M.; and Brox, T. 2019. Semi-supervised semantic segmentation with high-and low-level consistency. *IEEE transactions on pattern analysis and machine intelligence*.
- Miyato, T.; Maeda, S.-i.; Koyama, M.; and Ishii, S. 2018. Virtual adversarial training: a regularization method for supervised and semi-supervised learning. *IEEE transactions on pattern analysis and machine intelligence*, 41(8): 1979–1993.
- Odena, A. 2016. Semi-Supervised Learning with Generative Adversarial Networks. *arXiv:1606.01583*.
- Ouali, Y.; Hudelot, C.; and Tami, M. 2020a. An overview of deep semi-supervised learning. *arXiv preprint arXiv:2006.05278*.
- Ouali, Y.; Hudelot, C.; and Tami, M. 2020b. Semi-supervised semantic segmentation with cross-consistency training. In *Proceedings of the IEEE/CVF Conference on Computer Vision and Pattern Recognition*, 12674–12684.
- Park, N.; and Kim, S. 2021. How Do Vision Transformers Work? In *International Conference on Learning Representations*.
- Passalis, N.; and Tefas, A. 2018. Learning deep representations with probabilistic knowledge transfer. In *Proceedings of the European Conference on Computer Vision (ECCV)*, 268–284.
- Peng, B.; Jin, X.; Liu, J.; Li, D.; Wu, Y.; Liu, Y.; Zhou, S.; and Zhang, Z. 2019. Correlation congruence for knowledge distillation. In *Proceedings of the IEEE/CVF International Conference on Computer Vision*, 5007–5016.
- Raghu, M.; Unterthiner, T.; Kornblith, S.; Zhang, C.; and Dosovitskiy, A. 2021. Do Vision Transformers See Like Convolutional Neural Networks? *Advances in Neural Information Processing Systems*, 34.
- Ronneberger, O.; Fischer, P.; and Brox, T. 2015. U-net: Convolutional networks for biomedical image segmentation. In *International Conference on Medical image computing and computer-assisted intervention*, 234–241. Springer.
- Rosenberg, C.; Hebert, M.; and Schneiderman, H. 2005. Semi-Supervised Self-Training of Object Detection Models. In *2005 Seventh IEEE Workshops on Applications of Computer Vision (WACV/MOTION'05) - Volume 1*, volume 1, 29–36.
- Saito, K.; Kim, D.; and Saenko, K. 2021. OpenMatch: Open-Set Semi-supervised Learning with Open-set Consistency Regularization. In Beygelzimer, A.; Dauphin, Y.; Liang, P.; and Vaughan, J. W., eds., *Advances in Neural Information Processing Systems*.
- Sajjadi, M.; Javanmardi, M.; and Tasdizen, T. 2016. Regularization With Stochastic Transformations and Perturbations for Deep Semi-Supervised Learning. *arXiv:1606.04586*.
- Sohn, K.; Berthelot, D.; Li, C.-L.; Zhang, Z.; Carlini, N.; Cubuk, E. D.; Kurakin, A.; Zhang, H.; and Raffel, C. 2020. Fixmatch: Simplifying semi-supervised learning with consistency and confidence. *arXiv preprint arXiv:2001.07685*.
- Souly, N.; Spampinato, C.; and Shah, M. 2017. Semi Supervised Semantic Segmentation Using Generative Adversarial Network. In *Proceedings of the IEEE International Conference on Computer Vision (ICCV)*.
- Sun, Z.; Cao, S.; Yang, Y.; and Kitani, K. M. 2021. Rethinking transformer-based set prediction for object detection. In *Proceedings of the IEEE/CVF International Conference on Computer Vision*, 3611–3620.
- Szegedy, C.; Vanhoucke, V.; Ioffe, S.; Shlens, J.; and Wojna, Z. 2016. Rethinking the inception architecture for computer vision. In *Proceedings of the IEEE conference on computer vision and pattern recognition*, 2818–2826.

- Tarvainen, A.; and Valpola, H. 2017. Mean teachers are better role models: Weight-averaged consistency targets improve semi-supervised deep learning results. *Advances in neural information processing systems*, 30.
- Tian, Y.; Krishnan, D.; and Isola, P. 2019. Contrastive representation distillation. *arXiv preprint arXiv:1910.10699*.
- Touvron, H.; Cord, M.; Douze, M.; Massa, F.; Sablayrolles, A.; and Jégou, H. 2021. Training data-efficient image transformers & distillation through attention. In *International Conference on Machine Learning*, 10347–10357. PMLR.
- Vaswani, A.; Shazeer, N.; Parmar, N.; Uszkoreit, J.; Jones, L.; Gomez, A. N.; Kaiser, Ł.; and Polosukhin, I. 2017. Attention is all you need. In *Advances in neural information processing systems*, 5998–6008.
- Verma, V.; Lamb, A.; Kannala, J.; Bengio, Y.; and Lopez-Paz, D. 2019. Interpolation Consistency Training for Semi-Supervised Learning. In *IJCAI*.
- Wang, J.; Sun, K.; Cheng, T.; Jiang, B.; Deng, C.; Zhao, Y.; Liu, D.; Mu, Y.; Tan, M.; Wang, X.; et al. 2020a. Deep high-resolution representation learning for visual recognition. *IEEE transactions on pattern analysis and machine intelligence*, 43(10): 3349–3364.
- Wang, L.; and Yoon, K.-J. 2021. Knowledge distillation and student-teacher learning for visual intelligence: A review and new outlooks. *IEEE Transactions on Pattern Analysis and Machine Intelligence*.
- Wang, W.; Xie, E.; Li, X.; Fan, D.-P.; Song, K.; Liang, D.; Lu, T.; Luo, P.; and Shao, L. 2021a. Pyramid vision transformer: A versatile backbone for dense prediction without convolutions. *arXiv preprint arXiv:2102.12122*.
- Wang, Y.; Wang, H.; Shen, Y.; Fei, J.; Li, W.; Jin, G.; Wu, L.; Zhao, R.; and Le, X. 2022. Semi-Supervised Semantic Segmentation Using Unreliable Pseudo-Labels. In *Proceedings of the IEEE/CVF Conference on Computer Vision and Pattern Recognition*, 4248–4257.
- Wang, Y.; Xu, Z.; Wang, X.; Shen, C.; Cheng, B.; Shen, H.; and Xia, H. 2021b. End-to-end video instance segmentation with transformers. In *Proceedings of the IEEE/CVF Conference on Computer Vision and Pattern Recognition*, 8741–8750.
- Wang, Y.; Zhou, W.; Jiang, T.; Bai, X.; and Xu, Y. 2020b. Intra-class feature variation distillation for semantic segmentation. In *European Conference on Computer Vision*, 346–362. Springer.
- Wu, B.; Xu, C.; Dai, X.; Wan, A.; Zhang, P.; Yan, Z.; Tomizuka, M.; Gonzalez, J.; Keutzer, K.; and Vajda, P. 2020. Visual transformers: Token-based image representation and processing for computer vision. *arXiv preprint arXiv:2006.03677*.
- Xiong, B.; Fan, H.; Grauman, K.; and Feichtenhofer, C. 2021. Multiview Pseudo-Labeling for Semi-Supervised Learning From Video. In *Proceedings of the IEEE/CVF International Conference on Computer Vision (ICCV)*, 7209–7219.
- Yang, L.; Zhuo, W.; Qi, L.; Shi, Y.; and Gao, Y. 2022. St++: Make self-training work better for semi-supervised semantic segmentation. In *Proceedings of the IEEE/CVF Conference on Computer Vision and Pattern Recognition*, 4268–4277.
- Yang, M.; Yu, K.; Zhang, C.; Li, Z.; and Yang, K. 2018. Denseaspp for semantic segmentation in street scenes. In *Proceedings of the IEEE conference on computer vision and pattern recognition*, 3684–3692.
- Zhang, B.; Wang, Y.; Hou, W.; Wu, H.; Wang, J.; Okumura, M.; and Shinozaki, T. 2021. Flexmatch: Boosting semi-supervised learning with curriculum pseudo labeling. *Advances in Neural Information Processing Systems*, 34.
- Zheng, S.; Lu, J.; Zhao, H.; Zhu, X.; Luo, Z.; Wang, Y.; Fu, Y.; Feng, J.; Xiang, T.; Torr, P. H.; et al. 2021. Rethinking semantic segmentation from a sequence-to-sequence perspective with transformers. In *Proceedings of the IEEE/CVF Conference on Computer Vision and Pattern Recognition*, 6881–6890.
- Zhu, X.; Su, W.; Lu, L.; Li, B.; Wang, X.; and Dai, J. 2020. Deformable detr: Deformable transformers for end-to-end object detection. *arXiv preprint arXiv:2010.04159*.
- Zou, Y.; Zhang, Z.; Zhang, H.; Li, C.-L.; Bian, X.; Huang, J.-B.; and Pfister, T. 2020. Pseudoseg: Designing pseudo labels for semantic segmentation. *arXiv preprint arXiv:2010.09713*.